The effect of pressure overload and pressure unloading of the left ventricle on cardiac structure and function

PhD thesis

Mihály Ruppert, M.D.

Doctoral School of Basic and Translational Medicine

Semmelweis University

Supervisor: Tamás Radovits M.D., Ph.D

Official reviewers: József Kaszaki M.D., Ph.D.
Anikó Görbe M.D., Ph.D.

Head of the Complex Examination Committee:
Tivadar Tulassay, M.D., D.Sc.

Members of the Complex Examination Committee:
Attila Patócs, M.D., D.Sc.
Péter Andréka, M.D., Ph.D.

Budapest
2020

Introduction

Chronic heart failure (CHF) represents the most rapidly growing cardiovascular condition worldwide in the twenty-first century. Notably, a wide range of pathological conditions can lead to the development of CHF. Among them, ischemic heart disease and primary/secondary cardiomyopathies are often associated with irreversible myocardial insult. In contrast, a great body of scientific evidence have confirmed that in pressure overload ([PO], aortic stenosis [AS] or arterial hypertension)-induced CHF termination of the hemodynamic overload could result in a state of reverse remodeling with substantial improvement in cardiac structure and function. Nevertheless, it has also been recognized that not all the patients experience the same extent of functional and structural recovery following pressure unloading therapy. Hence, efforts have been taken to identify factors which might affect the process of myocardial reverse remodeling.

One of these influential factors have been suggested to be the time point of medical interventions. This is underpinned by the fact that different ultrastructural alterations could be observed during the progression of PO-induced left ventricular (LV) hypertrophy (LVH). Accordingly, at a relatively early stage of PO-evoked LVH, cardiomyocyte hypertrophy and relatively low level of myocardial fibrosis could be detected. In contrast, at later stages of LVH, cardiomyocyte hypertrophy is accompanied by robust accumulation of myocardial interstitial and perivascular fibrosis. Importantly, it has been shown that the plasticity of myocardial fibrosis is substantially less than that of cardiomyocyte hypertrophy. Therefore, during the progression of PO-induced LVH, the structural alterations become less reversible. Concerning that an incomplete structural reverse remodeling could hamper the recovery of LV function, it has been suggested that patients might benefit more from earlier interventions. However, current guidelines recommend aortic valve replacement only in case of severe AS, when CHF symptoms are present and/or left ventricular systolic function is reduced (ejection fraction [EF]<50%). Therefore, further experimental evidence is warranted to support the notion that termination of the pathological stimulus of PO at earlier time points could result in a greater structural and thereby functional improvement.

Besides, the timing of interventions, the sex of the patients has emerged as another factor that might determine the success of myocardial reverse remodeling. Accordingly, recent clinical data indicate that women undergo a more complete reverse remodeling

after surgical/interventional aortic valve replacement, entailing better long-term outcomes. The more favorable therapeutic response to pressure unloading could be explained by the more physiological (and thereby more reversible) phenotype of PO-induced LVH among women. To be more specific, in female patients with long lasting arterial hypertension or AS, thicker ventricular walls, more concentric form of LVH and in particular less progressive fibrotic remodeling has been documented compared to their male counterparts. Besides the well-established structural differences, better preserved left ventricular systolic function has also been consistently reported in women with chronic PO. Nevertheless, it has to be mentioned that female sex also provides protection against many relevant co-morbidities, such as ischemic heart disease. As a consequence, making sex specific observations on fully identical populations in a clinical scenario is difficult. Therefore, further experimental studies are required to explore whether the documented disparities in LVH phenotype are indeed attributed to sex differences.

Objectives

Recent literature data have drawn the attention to the importance of different factors, which might influence the regression of PO-evoked LVH after pressure unloading. These findings have raised that possibility that the time point of medical interventions (performing pressure unloading at early versus late stages of PO-induced LVH) and the sex of the patients might be major determinants of myocardial reverse remodeling. Exploring the influential effects of these factors under standard, laboratory conditions could facilitate the optimization of the current recommendations for pressure unloading therapies.

Based upon that, the aims of the present studies were:

1. To establish a rat model of mechanical PO-induced pathological remodeling and pressure unloading-evoked reverse remodeling with microsurgical techniques.

2. To explore timeline alterations in left ventricular structure and function during the development of PO-induced LVH and its progression to CHF in male rats.

3. To investigate the effects of myocardial reverse remodeling from early versus late stages of PO-induced LVH in male rats.

4. To study the effect of sex on different aspects of left ventricular structure and function during the development of PO-induced LVH.

Methods

Animal models

Abdominal aortic banding (AB)

Following a one-week-long acclimatization period, banding of the abdominal aorta to the size of a 22-gauge-needle at the suprarenal level was carried out in male and female Sprague-Dawley rats (5-6 weeks-old; 160-180g; Janvier, France) under isoflurane anesthesia. Sham-operated animals were subjected to the same surgical procedure, except the aortic constriction

Debanding

After 6 weeks of AB (early debanding) or 12 weeks of AB (late debanding) a group of AB animals underwent a second minimal invasive surgery, when the aortic constriction was removed from the abdominal aorta (debanding) under isoflurane anesthesia.

Study protocols

Study 1: Longitudinal assessment of PO-induced LVH in male rats

The time points of week 6, 12 and 18 were chosen to detect characteristic alterations at early and advanced stages of PO-induced LVH.

Sham-wk6 (n=9): after sham operation the rats were followed-up for 6 weeks;

AB-wk6 (n=13): after AB the rats were followed-up for 6 weeks;

Sham-wk12 (n=9): after sham operation the rats were followed-up for 12 weeks;

AB-wk12 (n=13): after AB the rats were followed-up for 12 weeks;

Sham-wk18 (n=10): after sham operation the rats were followed-up for 18 weeks;

AB-wk18 (n=13): after AB the rats were followed-up for 18 weeks, respectively.

Study 2: Investigating the effect of early versus late pressure unloading

In this study, an early and a late debanded groups were added to the experimental protocol of Study 1.

Sham-wk6 (n=10): after sham operation the rats were followed-up for 6 weeks;

AB-wk6 (n=10): after AB the rats were followed-up for 6 weeks;

Sham-wk12 (n=10): after sham operation the rats were followed-up for 12 weeks;

AB-wk12 (n=11): after AB the rats were followed-up for 12 weeks;

Sham-wk18 (n=9): after sham operation the rats were followed-up for 18 weeks;

AB-wk18 (n=13): after AB the rats were followed-up for 18 weeks, respectively.

Early debanded (n=14); these rats underwent AB operation, after week 6 the banding suture was removed and the animals were followed up until week 12;

Late debanded (n=15): these rats underwent AB operation, after week 12 the banding suture was removed and the animals were followed up until week 18.

Study 3: Investigating sex-related differences in PO-induced LVH

Male and female rats underwent AB to investigate sex-related differences in the early and late stages of PO-induced LVH. Age- and sex-matched sham rats served as controls.

Male sham-wk6 (n=8): male sham-operated rats were followed-up for 6 weeks

Male AB-wk6 (n=8): male AB rats were followed-up for 6 weeks;

Female sham-wk6 *(n=8)*: female sham-operated rats were followed-up for 6 weeks

Female AB-wk6 (n=7): female AB rats were followed-up for 6 weeks;

Male sham-wk12 (n=8): male sham-operated rats were followed-up for 12 weeks;

Male AB-wk12 (n=10): male AB rats were followed-up for 12 weeks;

Female sham-wk12 (n=8): female sham-operated rats were followed-up for 12 weeks;

Female AB-wk12 (n=7): female AB rats were followed-up for 12 weeks.

Echocardiography

Echocardiography was carried out at baseline and at week 3, 6, 9, 12, 15 and 18 under isoflurane anesthesia. LV internal diameters (LV end-diastolic diameter [LVEDD] and LV end-systolic diameter [LVESD]) and anterior (AWT) and posterior wall thickness (PWT) values in diastole (d) and systole (s) were measured and LVmass and its index to body weight (LVmass index) and relative wall thickness (RWT) values were calculated.

LV pressure-volume analysis

At the end of the experimental period (at week 6, 12 or 18, respectively) invasive hemodynamic investigation was performed under isoflurane anesthesia. The following parameters were measured: systolic arterial blood pressure (SBP), diastolic arterial blood pressure (DBP), mean arterial pressure (MAP), heart rate (HR), LV end-systolic pressure (LVESP), LV end-diastolic pressure (LVEDP), maximal slope of systolic pressure increment (dP/dt_{max}) and diastolic pressure decrement (dP/dt_{min}), LV end-diastolic volume (LVEDV), LV end-systolic volume (LVESV), stroke volume (SV), cardiac

output (CO), ejection fraction (EF), arterial elastance (E_a; calculated by the following equation E_a=LVESP/SV), and time constant of LV pressure decay (Tau; according to the Glanz method) were computed and calculated. The slope of the end-systolic P-V relationship (ESPVR, according to the parabolic curvilinear model) and preload recruitable stroke work (PRSW) and the slope of the dP/dt_{max}-end-diastolic volume relationship (dP/dt_{max}-EDV) were calculated as reliable indices of LV contractility. To characterize myocardial compliance, the slope of the end-diastolic P-V relationship (EDPVR) was calculated. Furthermore, ventriculo-arterial coupling (VAC) was also assessed as the ratio of E_a and ESPVR (VAC= E_a/ESPVR). From the hemodynamic and echocardiographic measurements, LV meridional wall stress (σ) was estimated by the following equation (σ= 0.334*LVESP*[LVESD/(1+PWTs/LVESD)]).

Morphometry

After completion of the hemodynamic measurements, animals were euthanized by exsanguination and the organs were perfused in situ oxygenated Ringer solution to eliminate erythrocytes from myocardial tissue. Then, heart weights (HW) and tibial lengths (TL) were quickly measured. The ratio of heart weight-to-tibial length (HW/TL) was calculated to assess the extent of LVH.

LV histology

Transverse, transmural, 5-µm thick slices of the paraffin-embedded heart samples were cut and placed on adhesive slides. These sections were stained with hematoxylin and eosin and picrosirius red to determine cardiomyocyte diameter ([CD]) as a cellular marker of myocardial hypertrophy) and the extent of interstitial and perivascular collagen content, respectively.

LV gene expression analysis

LV myocardial samples stored at -80°C were homogenized in a lysis buffer and RNA was isolated. After measuring the quality and concentration of the isolated RNA, a reverse transcription reaction was carried out to produce cDNA samples. Quantitative real-time PCR was performed in duplicates to measure the mRNA expression levels of the following target genes: α-isoform of myosin heavy chain (α-MHC), β-isoform of myosin heavy chain (α-MHC), atrial type natriuretic peptide (ANP) and connective tissue growth factor (CTGF). Gene expression data was normalized to glyceraldehyde 3-phosphate

dehydrogenase (GAPDH), and expression levels were calculated using the CT comparative method ($2^{-\Delta CT}$). All results are expressed as values normalized to a positive calibrator ($[2^{-\Delta\Delta CT}]$).

LV protein expression analysis

LV samples stored at -80°C were homogenized in RIPA buffer containing protease inhibitors. Western blot measurement was performed to detect alterations in myocardial protein expression of CTGF. GAPDH housekeeping protein was used as loading control and protein normalization.

Statistical analysis

All values are expressed as mean±SEM. The distribution of the datasets was tested by D'Agostino-Pearson omnibus test, Shapiro-Wilk test or Kolmogorov-Smirnov test, depending on the number of measurements.

An unpaired two-sided Student's t-test in case of normal distribution or Mann-Whitney U test in case of non-normal distribution was used to compare two independent groups. Repeated-measures one-way analysis of variance (ANOVA) or Friedman test was performed for comparing data of the echocardiographic measurements at different time points within a group (in Study 1). To examine intergroup differences, Holm-Sidak or Dunn's post hoc test was carried out.

One-way ANOVA followed by Tukey's post hoc test or Kruskal-Wallis test followed by Dunn's post hoc test was carried out to compare three independent groups (in Study 2). Two-way ANOVA were carried out to compare six (in Study 1) or four (in Study 3) independent groups. Tukey post hoc test was utilized to detect intergroup differences.

A P value of <0.05 was used as a criterion for statistical difference. Furthermore, two additional categories ($P<0.01$ and $P<0.001$) were introduced to indicate the strength of the observed statistical difference.

Results

I. Longitudinal assessment of PO-induced LVH in male rats

Echocardiography

From week 3 until the end of the experimental period, AWTd, PWTd and $LVmass_{index}$ were increased in the AB-wk18 group compared to the sham-wk18 group, indicating the development of LVH. Furthermore, at week 12, week 15 and week 18, LVEDD was also increased in the AB-wk18 group compared to the sham-wk18 group, suggesting chamber dilatation.

Pathological hypertrophy and fibrosis markers

In the AB-wk6, AB-wk12 and AB-wk18 groups, HW/TL, CD and mRNA levels of β/α-MHC ratio and ANP were elevated compared to the corresponding sham groups. Furthermore, interstitial collagen area was also increased the AB-wk12 and AB-wk18 groups compared to the age-matched sham groups, respectively.

LV function

Arterial loading. SBP, DBP and MAP were elevated in the AB groups compared to the corresponding sham groups, confirming increased PO proximal to AB (*Table 1*).

Load-dependent systolic parameters. EF did not differ in the AB-wk6 group compared to the Sham-wk6 group. In contrast, in the AB-wk12 and AB-wk18 groups, EF decreased significantly compared to the corresponding sham groups (*Table 1*).

Load-independent contractility parameters. In the AB-wk6 group, ESPVR, PRSW and dP/dt_{max}-EDV increased significantly compared to the sham-wk6 group, indicating increased LV contractility (*Fig. 1*). This contractility augmentation diminished in the AB-wk12 and AB-wk18 groups. Accordingly, the load-independent contractility parameters were significantly decreased in the AB-wk12 and AB-wk18 groups compared to the AB-wk6 group (*Fig. 1*). However, ESPVR and PRSW did not differ in the AB-wk12 and AB-wk18 groups compared to the sham-wk12 and sham-wk18 groups.

VAC. In the AB-wk6 group, the enhanced LV contractility (increased ESPVR) counterbalanced the elevated afterload (increased E_a), therefore VAC did not differ from the corresponding sham group. In contrast, in the AB-wk12 and AB-wk18 groups, the lack of compensatory LV contractility augmentation (reduced ESPVR values compared to AB-wk6) along with the elevated afterload (increased E_a) resulted in contractility-

afterload mismatch. Thus, the values of VAC were significantly higher in the AB-wk12 and AB-wk18 groups compared to that of the AB-wk6 group (*Table 1*).

Diastolic parameters. Tau was significantly prolonged in the AB-wk6, AB-wk12 and AB-wk18 groups compared to the corresponding sham groups. Furthermore, the slope of EDPVR increased in the AB-wk18 group compared to the sham-wk18 group (*Table 1*).

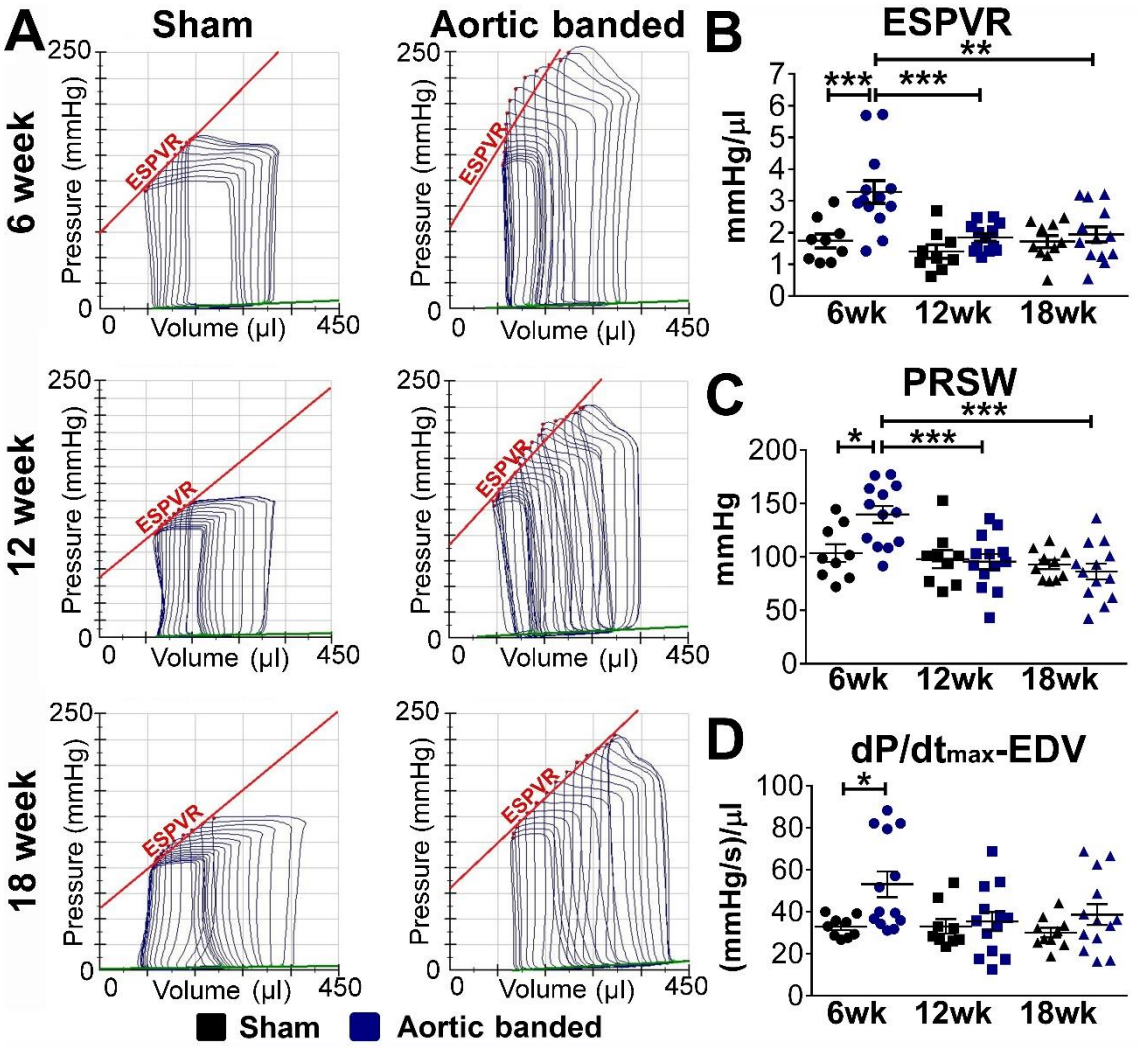

Figure 1. Alterations in left ventricular contractility during the progression of PO-induced pathological hypertrophy. A: Original pressure-volume loops were obtained at different preloads during transient vena cava occlusion. B, C, D: At week 6, the slope of the end-systolic P-V relationship (ESPVR), preload-recruitable stroke work (PRSW) and the slope of the dP/dt_{max}-end-diastolic volume relationship was increased in the aortic banded (AB) group, suggesting enhanced LV contractility. The contractility augmentation diminished at week 12 and 18 in the AB groups at week 12 and 18. *: P<0.05, **: P<0.01, ***: P<0.001.

Table 1. Hemodynamic parameters in aortic banded and sham-operated rats at different time points. Values are expressed as mean ± standard error of the mean. AB indicates aortic banding; SBP: systolic arterial blood pressure; DBP: diastolic arterial blood pressure; MAP: mean arterial pressure; HR: heart rate; LVEDV: left ventricular (LV) end-diastolic volume; LVESV: LV end-systolic volume; SV: stroke volume; CO: cardiac output; EF: ejection fraction, E_a: arterial elastance; VAC: ventriculo-arterial coupling; Tau: active relaxation time constant; EDPVR: end-diastolic pressure-volume relationship. *: P<0.05 vs. age-matched sham. **: P<0.01 vs. age-matched sham. ***: P<0.001 vs. age-matched sham. #: P<0.05 vs. AB-week 6## : P<0.01 vs. AB-week 6. ###: P<0.001 AB-week 6. $: P<0.05 vs. AB-week 12. $$: P<0.01 vs. AB-week 12.

	Week 6		**Week 12**		**Week 18**	
	Sham (n=9)	***AB*** (n=13)	***Sham*** (n=9)	***AB*** (n=13)	***Sham*** (n=10)	***AB*** (n=13)
SBP, mmHg	148±4	**215±4*****	138±5	**215±5*****	150±5	**228±4*****
DBP, mmHg	116±3	**150±2*****	110±4	**154±4*****	120±4	**170±3*****###$$**
MAP, mmHg	127±4	**172±2*****	119±4	**174±4*****	140±4	**189±3*****##$**
HR, beats/min	355±7	369±9	354±5	366±7	379±7	357±5
LVEDV, µl	268±16	305±14	286±23	320±20	283±18	327±14
LVESV, µl	175±15	194±12	178±17	231±11	160±11	**241±11*****
SV, µl	188±16	173±10	195±11	163±12	175±10	151±15
CO, ml/min	66.7±6.1	62.9±3.0	69.4±4.5	59.4±4.1	66.3±4.4	53.7±5.4
EF, %	58±3	51±2	57±2	**44±2****	55±2	**41±3*****##
E_a, mmHg/µl	0.75±0.06	**1.20±0.08***	0.68±0.05	**1.33±0.10*****	0.84±0.05	**1.54±0.16*****
VAC	0.50±0.08	0.45±0.06	0.54±0.06	**0.76±0.08##**	0.57±0.10	**0.87±0.08###**
Tau, ms	14.2±0.4	**18.4±0.9****	12.8±0.6	**19.4±0.6*****	13.0±0.3	**21.7±1.2*****#**
EDPVR, mmHg/µl	0.038±0.005	0.038±0.007	0.028±0.004	0.042±0.006	0.014±0.003	**0.032±0.004****

II. Investigating the effect of early versus late pressure unloading

Echocardiography

Both early and late debanding resulted in significant regression of LVmass, AWTd and PWTd (*Fig. 2*A-F). No differences could be observed in the extent of regression of the echocardiographic parameters between the early and late debanded groups (*Fig. 2G-I*).

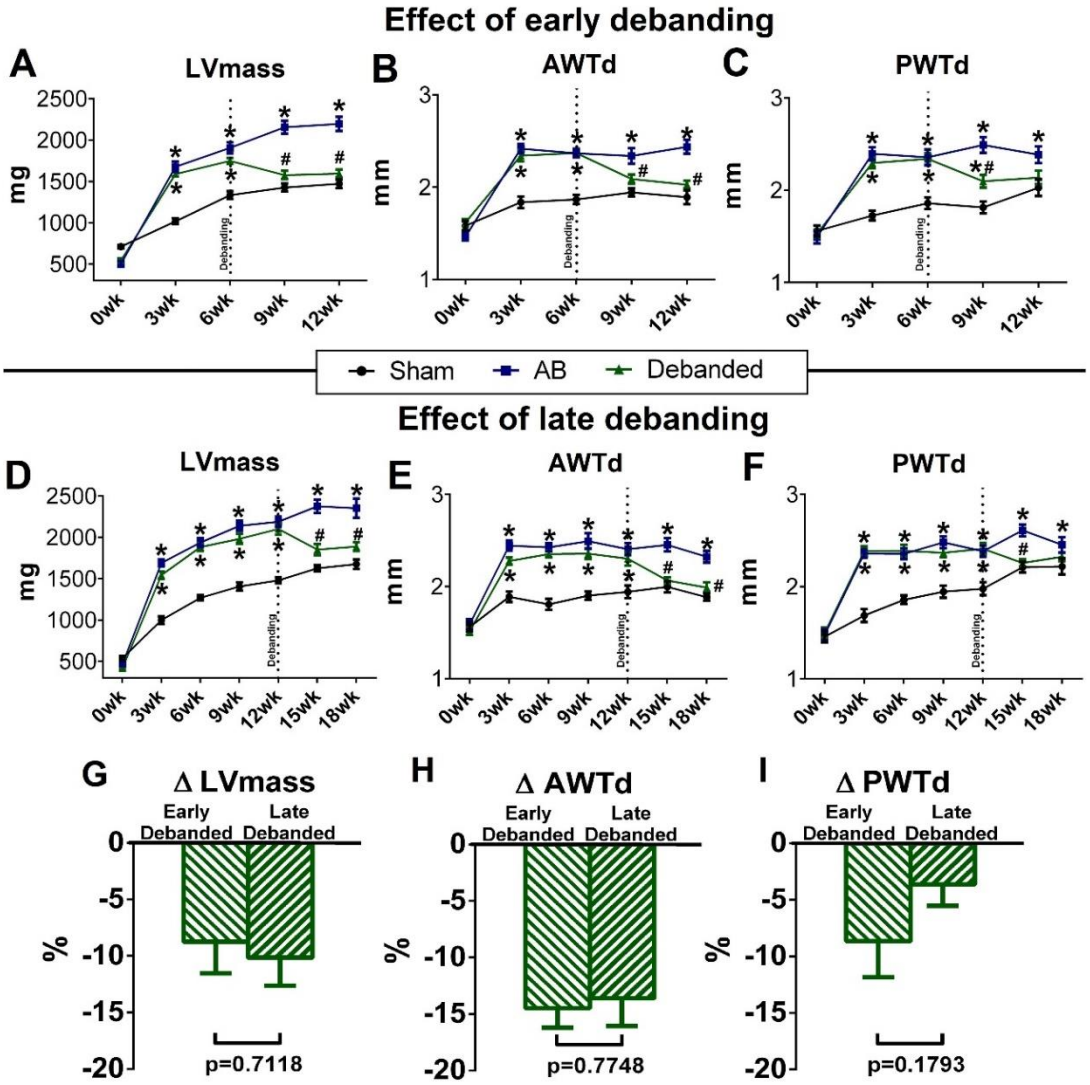

Figure 2. Echocardiographic follow-up during myocardial reverse remodeling from early- and late-stage of pathological hypertrophy. Both in the early and in the late debanded groups**,** left ventricular (LV) mass (LVmass) (A, D), anterior wall thickness measured in diastole (AWTd) (B, E) and posterior wall thickness measured in diastole (PWTd) (C, F) effectively regressed after pressure unloading. No differences could be observed in the extent of LVmass (G), AWTd (H) and PWTd (I) regression. AB indicates aortic banded. *: P < 0.05 vs. age-matched sham. #: P<0.05 vs. age-matched AB.

Pathological hypertrophy and fibrosis markers

Both in the early and in the late debanded groups, CD, HW/TL and the re-expression of the fetal gene program (as reflected by β/α-MHC ratio) were decreased compared to the age-matched AB groups. Regarding CD, HW/TL and β/α-MHC, no differences could be detected in the extent of regression between the early and the late debanded groups.

Furthermore, in the early debanded group interstitial and perivascular fibrosis also decreased compared to the age-matched AB group (*Fig. 3A-B*). However, in the late debanded group, interstitial and perivascular fibrosis remained increased, and it did not differ from the age-matched AB group (*Fig. 3C-D*). Accordingly, the extent of both interstitial and perivascular fibrosis showed significantly higher levels in the late debanded group compared to the early debanded group (*Fig. 3E-F*).

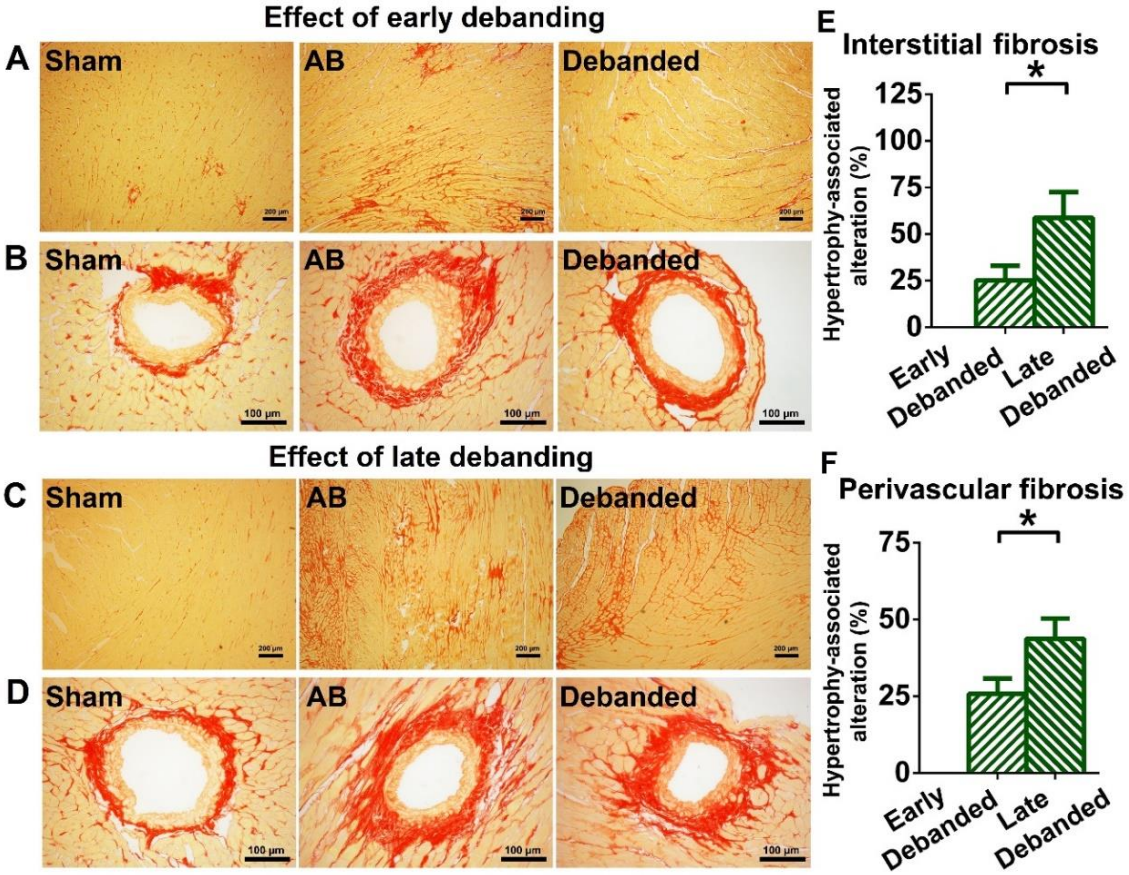

Figure 3. Effect of early and late pressure unloading on myocardial fibrosis. Representative photomicrographs of picrosirius red staining are shown demonstrating interstitial fibrosis (A, C) (magnification 50x, scale bar: 200µm) and perivascular fibrosis (B, D) (magnification 100x, scale bar: 100µm). Both interstitial and perivascular fibrosis regressed to a greater extent in the early debanded group compared to the late debanded group (E, F). AB indicates aortic banded. *: P<0.05

LV function

Arterial loading and meridional wall stress. In the early and late debanded groups, SBP, DBP, MAP and σ decreased compared to the age-matched AB groups. The extent of afterload and wall stress reduction did not differ between the two debanded groups.

Load-dependent systolic parameters. Both in the early and in the late debanded groups EF increased compared to the age-matched AB groups. No differences were found regarding the extent of improvement in EF between the two debanded groups.

Load-independent contractility parameters. ESPVR and PRSW did not differ in the early or late debanded groups compared to their corresponding AB groups (*Figure 4*).

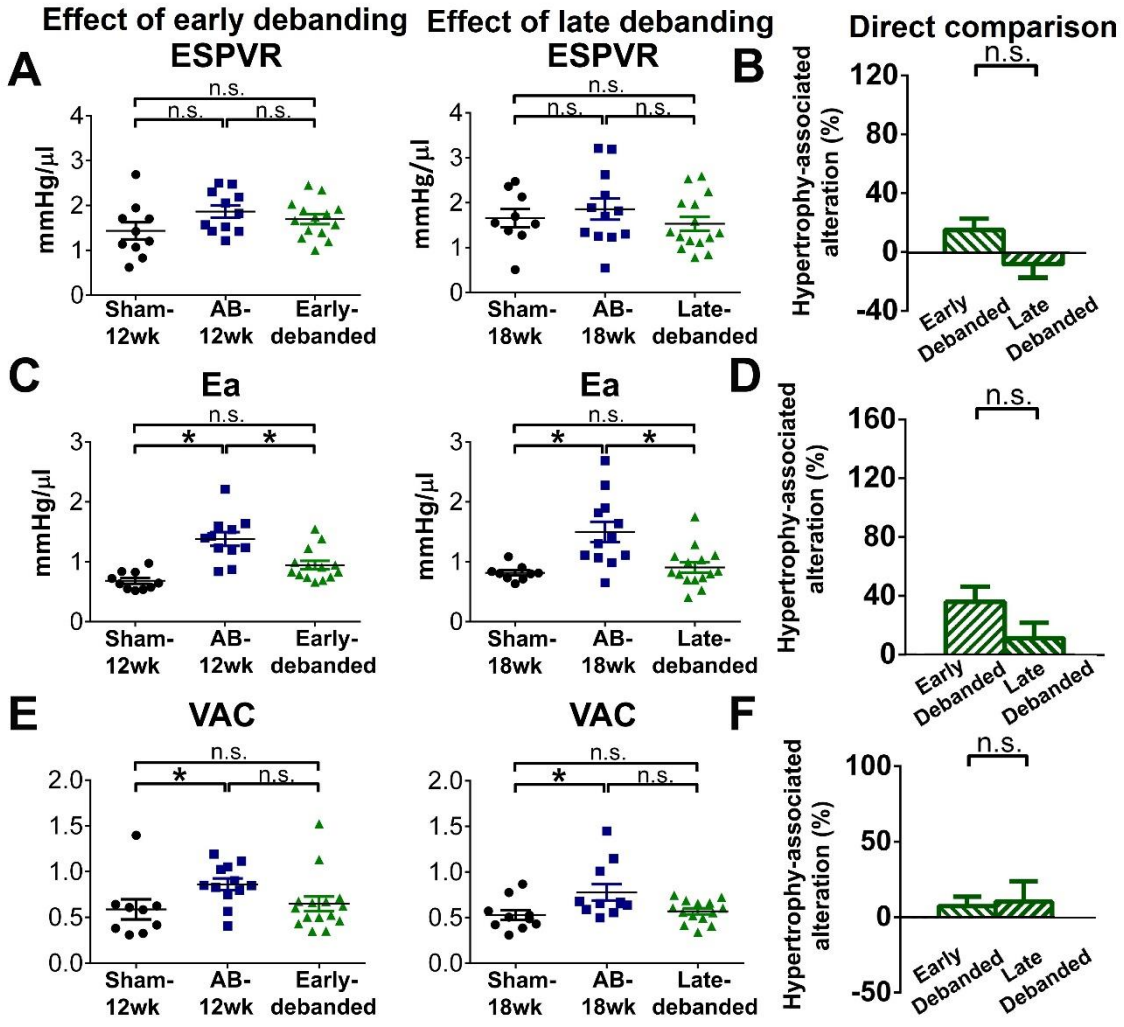

Figure 4. The effect of early and late debanding on ventriculo-arterial coupling (VAC). A-B: Pressure unloading had no effect on left ventricular contractility (expressed as the slope of end-systolic pressure-volume relationship [ESPVR]). C-D: In contrast, both early and late debanding effectively reduced arterial elastance (E_a). E-F: Thereby, VAC was normalized to the same extent in the debanded groups. *: P<0.05

VAC. Both in the early- and in the late debanded groups, reduction of E_a efficiently normalized the relation of the LV contractility and the connecting arterial system and resulted in adequate VAC values (*Fig. 4C, E*). No differences could be observed in the extent of VAC normalization between the early and the late debanded groups (*Fig. 4F*).

Diastolic function. In the early debanded group, the prolonged active relaxation (Tau) was effectively shortened. (*Fig. 5A*). In the late debanded group, Tau was also decreased compared to the age-matched AB group (*Fig. 5A*). However, the extent of improvement was smaller compared to the early debanded group (*Fig. 5B*). Furthermore, in the early debanded group, LV stiffness decreased compared to the corresponding AB group (*Fig. 5C*). In contrast, no significant differences could be observed in EDPVR between the late debanded group and the AB-wk18 group (*Fig. 5C*). Thus, the extent of improvement in LV stiffness was smaller in late debanded than that observed in early debanded (*Fig. 5D*).

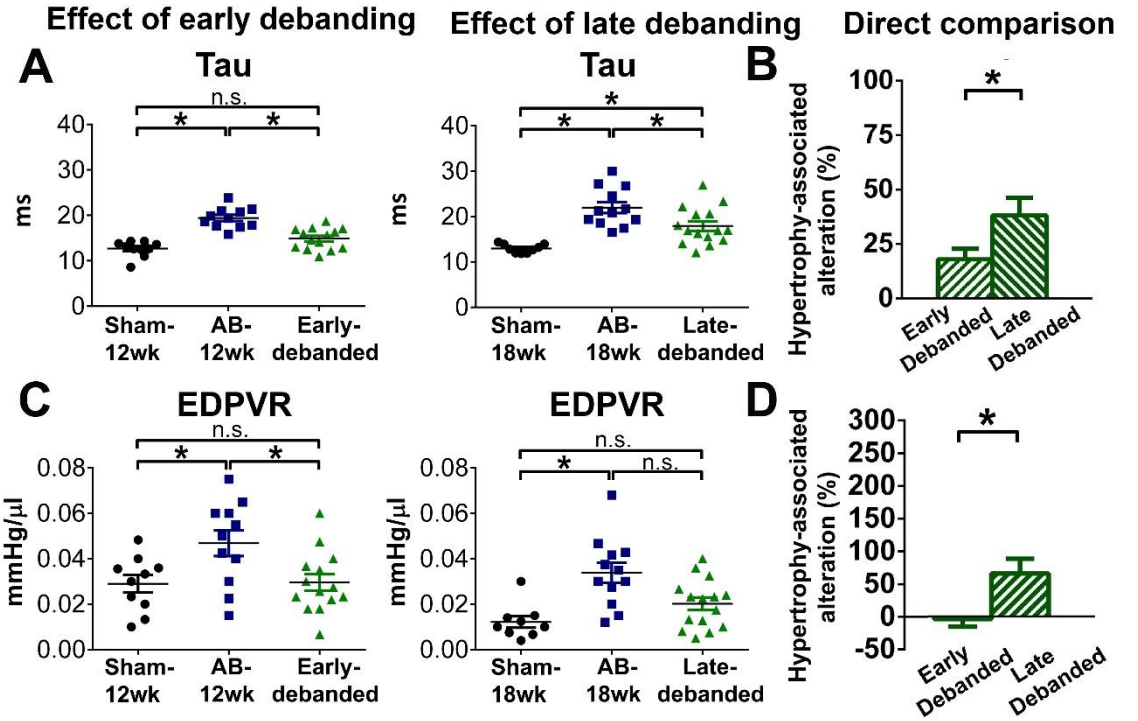

Figure 5. The effect of early and late debanding on diastolic function. Active relaxation (expressed as Tau) and ventricular stiffness (expressed as the slope of the end-diastolic pressure-volume relationship [EDPVR]) were improved in the early debanded group (A, C). In contrast, late debanded failed to normalize diastolic dysfunction. Accordingly, robust differences were observed between the early and the late debanding groups in Tau and EDPVR (B, D). *: P<0.05

III. Investigating sex-related differences in PO-induced LVH

Echocardiography

LVmass index increased in both male and female AB rats from week 3 until the end of the experimental period (*Fig. 6A-B*). RWT revealed concentric LV geometry at week 6 in both male and female AB groups (*Fig. 6C*). Concentric geometry was also observed in female AB rats at week 12. However, at week 12, RWT substantially decreased in male AB rats, leading to eccentric LV geometry (*Fig. 6C*).

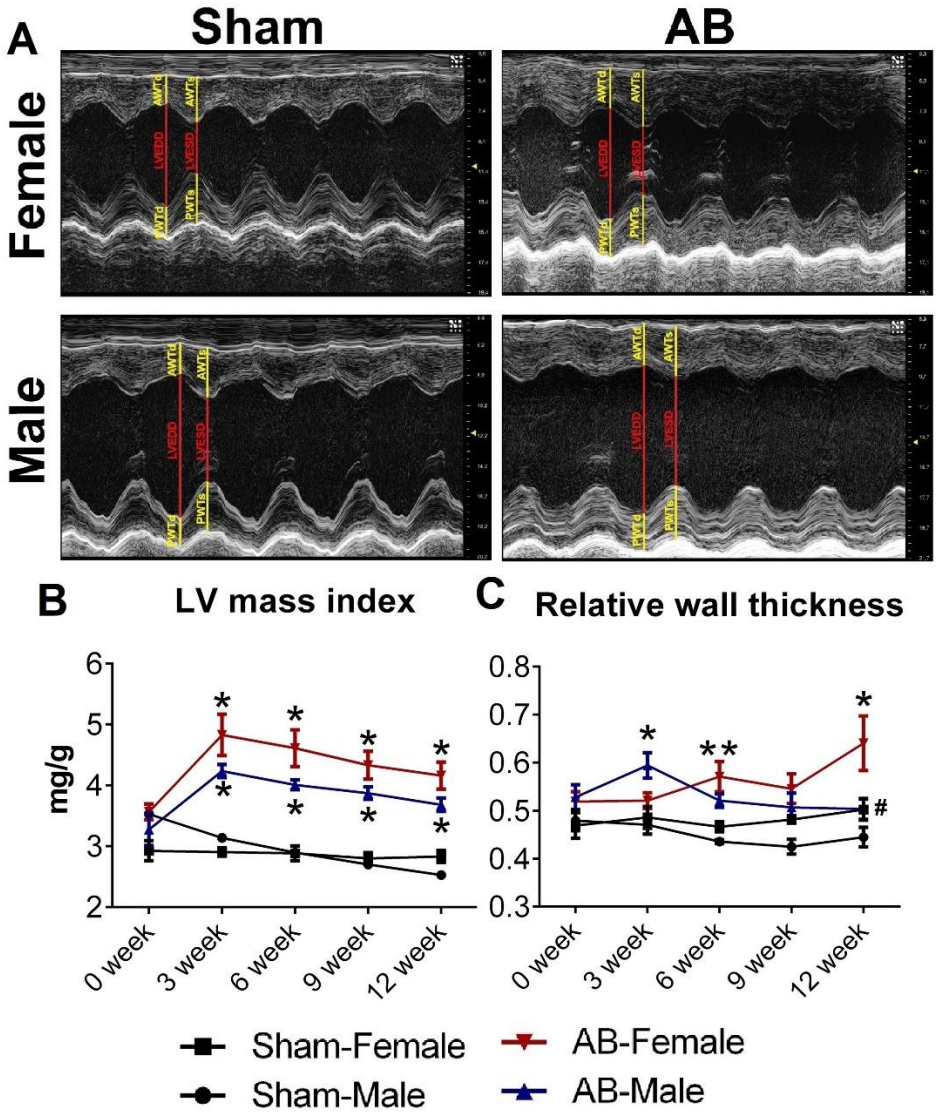

Figure 6. Sex-related differences in pathological hypertrophy between male and female aortic banded (AB) rats. A: Representative echocardiographic recordings are shown at week 12. B: LVmass index increased in both male and female AB rats, confirming the development of LVH. C: At week 12, relative wall thickness indicated concentric left ventricular (LV) geometry in female AB rats, and eccentric LV geometry in male AB rats. *: P<0.05 vs. age and sex-matched sham. #: P<0.05 vs. female AB.

Pathological hypertrophy and fibrosis markers

At week 6 HW/TL, CD, myocardial collagen area and CTGF mRNA levels were enhanced in both male and female AB rats compared to their age- and sex-matched sham groups. The extent of hypertrophy and fibrosis was comparable between the two sexes at this early time point. At week 12 the hypertrophy and fibrosis markers were also increased in male and female AB rats compared to their corresponding sham groups. However, the direct comparison of sexes revealed higher increments in HW/TL and CD in females compared to males. In contrast, fibrosis showed significant progression from week 6 to week 12 only in male AB rats. Furthermore, the extent of AB-associated increment in CTGF expression was also significantly higher in males compared to females.

LV function

Arterial loading. At week 6 and 12, in both male and female AB rats increased SBP, DBP and MAP were confirmed.

Load-dependent systolic parameters. At week 6, the AB groups were associated with preserved EF in both sexes. In contrast at week 12, reduced EF could be detected in male but not in female AB groups compared to their corresponding sham groups.

Load-independent contractility parameters. At week 6, the load-independent indices of cardiac contractility (PRSW and ESPVR) were significantly increased in both male and female AB groups when compared to their control groups (*Fig. 7*). The direct comparison of the two sexes revealed no significant differences in the extent of contractility augmentation at this time point (*Fig. 7*). At week 12, a significant reduction from the 6-week state could be observed in PRSW and ESPVR among male AB rats. In contrast, in female animals, LV contractility remained increased, and PRSW and ESPVR were significantly higher when compared to the corresponding sham group (*Fig. 7*).

VAC. At week 6, augmentation in ESPVR counterbalanced the increment in E_a, resulting in preserved VAC ratio in the AB groups in both sexes. At week 12, reduction of contractility in male AB rats led to an impairment in the VAC ratio, On the contrary, the maintained contractility augmentation in female AB rats ensured preserved VAC ratio even after 12 weeks of PO.

Diastolic function. At week 6, the AB groups were associated with impaired active relaxation (prolonged Tau) in both sexes when compared to the corresponding sham

groups. The degree of Tau prolongation was similar between the two genders at this early stage of PO-induced LVH. At week 12, prolongation of Tau was also evident in both male and female AB rats. However, at this time, impairment of active relaxation occurred at a significantly greater extent in male AB rats. Furthermore, LVEDP and the slope EDPVR were consistently elevated in male but not in the female AB animals at week 12, leading to substantial differences between the two sexes.

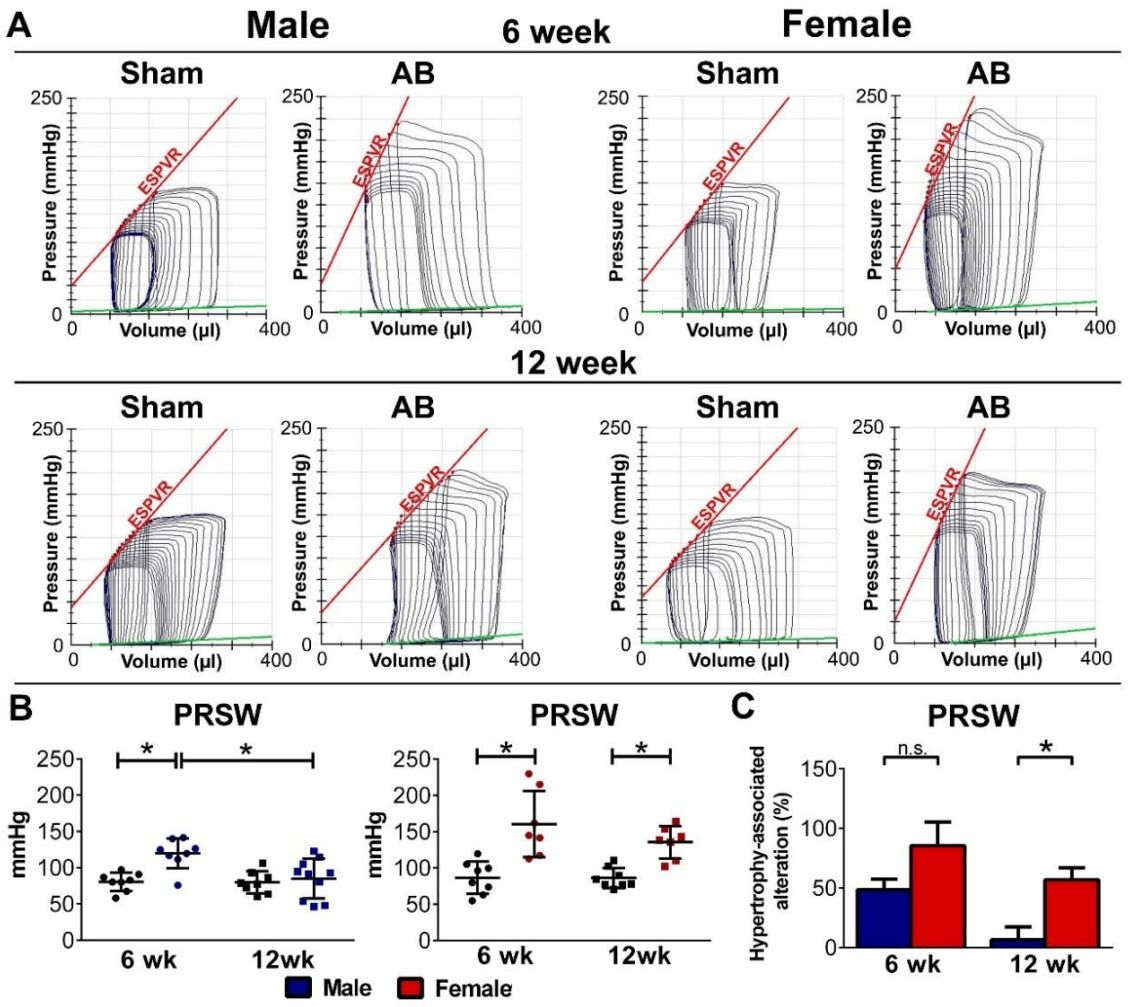

7. Sex-related differences in left ventricular contractility in aortic banded (AB) rats. A: Representative pressure-volume recordings during vena cava occlusion. The slope of the end-systolic pressure-volume relationship (ESPVR) indicates contractility. B-C: At week 6, preload recruitable stroke work (PRSW) was increased in both male and female AB rats. At week 12, the contractility augmentation was still present in the female AB group, however it diminished in the male AB group. Thus, at week 12, substantial difference could be observed in left ventricular contractility between the two sexes. *: $P<0.05$.

Conclusions

PO-induced pathological LVH regresses after pressure unloading. Nevertheless, it has been recognized that in some patients, LV dysfunction and CHF symptoms persist even after optimal medical therapy. Recent clinical data indicates that the time point of medical interventions and the sex of the patients might influence the regression of LVH. Hence, this study, we aimed to investigate the influential effects of this two particular factors.

One of the main conclusions of our experiments is that pressure unloading therapy at both early and late time points effectively improves LV systolic function. By performing invasive P-V analysis we confirmed that increased arterial afterload and not depressed LV contractility underpins the reduced systolic performance even at advanced stages of PO-induced LVH in the abdominal AB rat model. Hence, terminating the PO at both early and late time points rapidly normalizes the relation between the contractile state of the LV and the afterload of the connecting arterial system.

In contrast to systolic function, we found that diastolic function (both active relaxation and myocardial stiffness) recovers to a greater extent in case of early debanding compared to late debanding. This finding might be explained by the fact that the early pressure unloading therapy entailed a more complete structural reverse remodeling compared to the late-stage surgery. Accordingly, regression of reactive interstitial and perivascular fibrosis was only detected in the early debanded group, while it persisted in the late debanded group. These results call attention to the fact that performing pressure unloading therapy at an earlier time point may be superior in regard to normalization of diastolic function.

Furthermore, the sex of the patients has been also suggested to influence the outcome of pressure unloading therapies. Here, we confirmed that the advanced stage of PO-induced LVH is associated with less myocardial fibrosis as well as less severely impaired LV active relaxation and myocardial stiffness in female compared to male AB rats. As interstitial fibrosis and diastolic dysfunction have been found to be those factors, which display less reversibility after pressure unloading, our results might indicate that women could indeed experience a more complete functional reverse remodeling from late-stage LVH.

Bibliography of the candidate's publications

Publications related to the dissertation

I. **Ruppert M***, Bódi B*, Korkmaz-Icöz S, Loganathan S, Jiang W, Lehmann L, Oláh A, Barta BA, Sayour AA, Merkely B, Karck M, Papp Z, Szabó G, Radovits T. (2019) Myofilament Ca^{2+} sensitivity correlates with left ventricular contractility during the progression of pressure overload-induced left ventricular myocardial hypertrophy in rats. J Mol Cell Cardiol, 129:208-218.
IF: 5.055
*: equal contribution

II. **Ruppert M**, Korkmaz-Icöz S, Loganathan S, Jiang W, Oláh A, Sayour AA, Barta BA, Karime C, Merkely B, Karck M, Radovits T, Szabó G. (2019) Incomplete structural reverse remodeling from late-stage left ventricular hypertrophy impedes the recovery of diastolic but not systolic dysfunction in rats. J Hypertens, 37:1200-1212.
IF: 4.209

III. **Ruppert M**, Korkmaz-Icöz S, Loganathan S, Jiang W, Lehmann L, Oláh A, Sayour AA, Barta BA, Merkely B, Karck M, Radovits T, Szabó G. (2018) Pressure-volume analysis reveals characteristic sex-related differences in cardiac function in a rat model of aortic banding-induced myocardial hypertrophy. Am J Physiol Heart Circ Physiol, 315:H502-H511.
IF: 4.048

IV. **Ruppert M**, Bódi B, Nagy D, Korkmaz-Icöz S, Loganathan S, Oláh A, Barta BA, Sayour AA, Benke K, Karck M, Merkely B, Papp Z, Szabó G, Radovits T. (2019) A miofilamentáris rendszer Ca^{2+}-érzékenysége korrellál a bal kamrai kontraktilitással a fokozott nyomásterhelés által előidézett patológiás szívizom-hipertrófia patkánymodelljében. Cardiol Hung, 49: 88-99.